



Remote Sensing Technology Institute

**ATBD
DRAFT**

**Phytoplankton
classification**

Title: **Phytoplankton classification**

Doc. no: MAPP-ATBD-PCLASS

Issue: Draft

Revision: 0

Date: Friday, 4 February 2000

Author: Peter Gege

Organisation: DLR
Remote Sensing Technology Institute
P.O.Box 1116
D-82230 Wessling
Germany

internal Distribution

Name

Quantity

external Distribution

Name

Quantity


Change Record

Issue

RevisionDate


Description

Change pages

 <p>DLR Remote Sensing Technology Institute</p>	<p>ATBD Phytoplankton classification DRAFT</p>	<p>Doc. ID : MAPP-ATBD-PCLASS Name : Phytoplankton Classification Issue : Draft Rev.: 0 Date : 4.2.2000 Page : 1</p>
--	--	--

1. Introduction

This is a preliminary draft version of the ATBD "phytoplankton classification". The goal is to produce maps of the distribution of major phytoplankton classes from MERIS data. The corresponding MERIS processor had been defined at the beginning of the project as an experimental product, because it was not clear if the goal can be achieved. Earlier work had shown that from spectrally highly resolved reflectance spectra, which were measured onboard a ship, a distinction between four phytoplankton classes is possible and that the relative concentrations can be determined with a class-dependent accuracy between 12 and 25 % (Gege 1994, 1998b). During several campaigns within the MAPP project an extended data set was collected for improving the model. This draft reflects the work performed for improving the model; it is not yet at a stage to be applicable to MERIS.

 <p>DLR Remote Sensing Technology Institute</p>	<p>ATBD Phytoplankton classification DRAFT</p>	<p>Doc. ID : MAPP-ATBD-PCLASS Name : Phytoplankton Classification Issue : Draft Rev.: 0 Date : 4.2.2000 Page : 2</p>
--	--	--

2. Algorithm overview

Advanced remote sensing algorithms allow to determine the concentrations of three classes of water constituents: chlorophyll, yellow substance, and suspended matter (Schiller and Doerffer 1993, Krawczyk et al. 1993, Hoge and Lyon 1996). Two of these algorithms will be adapted to MERIS (ATBD WC1, WC2). They are based on physical models of the radiative transfer in the water, at the air-water-interface and in the atmosphere. These can be applied, in principle, to any type of water, while the widely used empirical algorithms are restricted to so-called case I waters, mainly open ocean areas, which are dominated by a single optical class of water constituents.


It is the goal of the present algorithm to refine the chlorophyll class, i.e. to distinguish between different phytoplankton classes and to determine their concentrations. This is realised by including additional classes of water constituents into a physical model of the radiative transfer. Phytoplankton classes are relatively similar in their optical properties compared to the spectral differences between chlorophyll, yellow substance and suspended matter, thus phytoplankton classification is much more sensitive on errors. At the present stage of the project it is still not clear how many phytoplankton classes can be distinguished using MERIS data, nor is it known if a satisfactory accuracy can be achieved. The two major challenges of the algorithm are:

- to find a parameterisation of the measured radiance spectra which is robust against errors;
- to define a representative and remote-sensing-suited classification of the numerous phytoplankton species.

The two tasks resulting from these challenges are to select and optimise the physical model that describes the water-leaving radiance spectrum, and to fill the data base. This requires an extensive data set that comprises remote sensing data (water leaving radiances and reflectances), optical data of the upper water layer (reflectance, attenuation, absorption, scattering, backscattering), biochemical data (concentrations of various phytoplankton pigments, dissolved organic matter (yellow substance) and inorganic suspended matter), taxonomic data (abundancies of phytoplankton species or classes), and absorption spectra of the most abundant phytoplankton classes. A suitable data set that comprises all required measurements was obtained during several campaigns at Lake Constance. It is the experimental basis of the proposed algorithm.

The algorithm is based on full-resolution MERIS Level-2 data, i.e. normalized water leaving radiance (reflectance) spectra. It is assumed that these have been corrected with sufficient accuracy from atmospheric influences by the ESA software. No emphasis is laid on optimising computing time, as this has been done by others for similar algorithms devoted to water constituents (ATBD WC1, WC2), and it is expected that an adaptation is possible.

Here follows in the final ATBD a short summary of the algorithm. The algorithm is not finished at the present stage of the project.

 <p>DLR Remote Sensing Technology Institute</p>	<p>ATBD Phytoplankton classification DRAFT</p>	<p>Doc. ID : MAPP-ATBD-PCLASS Name : Phytoplankton Classification Issue : Draft Rev.: 0 Date : 4.2.2000 Page : 3</p>
--	--	--

3. Algorithm Description

3.1 Theoretical Description

3.1.1 Physics of the Problem

A radiance sensor pointing from low altitude (ship) towards the water surface detects the sum L_u of two radiation components originating from the water: a component L_s from the surface and a component L_w from the water body:

$$L_u(\lambda) = L_w(\lambda) + L_s(\lambda). \quad (1)$$


At high altitude (aircraft, satellite) L_u is modified due to absorption and scattering processes in the atmosphere. It is the task of atmosphere correction algorithms to correct these modifications, see 5.1.

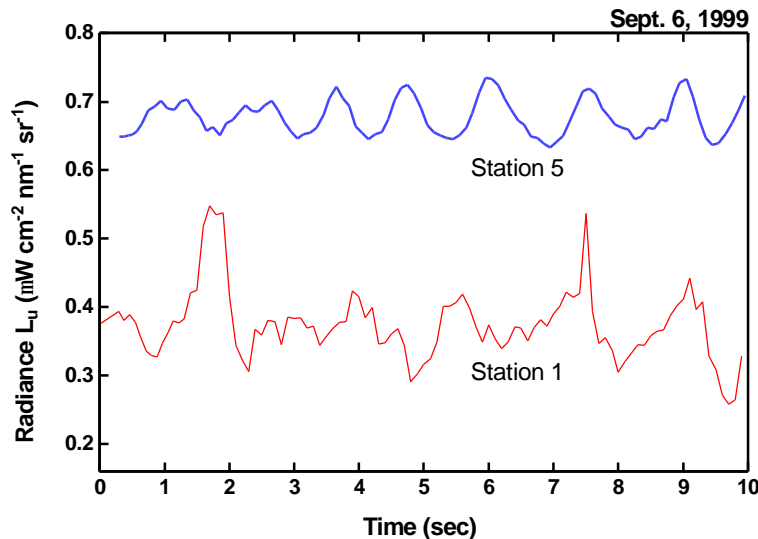
3.1.1.1 Specular reflections at the water surface

Reflection at the water surface obeys to the Fresnel equations. The radiation which is reflected at a smooth water surface from the sky into a radiance sensor is the radiance $L_d(\theta, \phi)$ downwelling from zenith angle θ and azimuth angle ϕ , multiplied with the Fresnel reflectance $\sigma(\theta)$:

$$L_s(\lambda, \pi-\theta, \pi+\phi) = \sigma(\theta) \cdot L_d(\lambda, \theta, \phi). \quad (2)$$

If the water surface is wind-roughened, radiance from any point in the sky can in principle be reflected by the wavy surface into the sensor. In this case $\sigma(\theta)$ becomes a function of time, wavelength, wind speed, the sky radiance distribution and the sensor's field of view. The temporal variability of L_u is illustrated in Fig. 1. A typical value of $\sigma(\theta)$ is 0.028 for a viewing direction which minimizes the effect of sunglint (40° from the nadir and 135° from the sun) for wind speeds less than 5 m/s (Mobley 1999).

 <p>DLR Remote Sensing Technology Institute</p>	<p align="center">ATBD Phytoplankton classification DRAFT</p>	<p>Doc. ID : MAPP-ATBD-PCLASS Name : Phytoplankton Classification Issue : Draft Rev.: 0 Date : 4.2.2000 Page : 4</p>
--	---	--



GLINTVAR | 11.1.2000


Fig. 1: Temporal variation of the upwelling radiance L_u (average from 400 to 700 nm) at two stations at Lake Constance for a slightly wind-roughened water surface. The curves show 100 measurements à 12 ms integration time. At station 1 cloud cover was variable, at station 5 the sky around the sun was cloud-free.

In Fig. 1 the variability of L_u is caused by the variability of L_s . For ship measurements it can be reduced, in principle, by extending the integration time to few seconds. Spatial averaging, which is system immanent for sensors on aircrafts and satellites, also reduces the variability. The average L_s value is correlated with wind speed (Cox and Munk 1954) and wind direction (Cox and Munk 1956). These Cox-Munk relations are usually taken for correcting specular reflections at the water surface for remote sensing data. However, when applied to data with spatial or temporal variability of L_s or for unknown wind speed, the remaining error may be significant. Since more light may be reflected at the surface than in the water for certain observation conditions, these errors can be very critical for determining the concentrations of water constituents.

Because correction of the reflections at the water surface is very important and the standard algorithm based on the Cox-Munk relations is not accurate enough for many situations, alternate algorithms have been developed for measurements from ship (Gege 1998a) and aircraft (Heege 2000). These will be applied to MERIS data and validation measurements. They are described below.

3.1.1.2 Transmission across the air-water boundary

Only few percent of the downwelling radiation are specularly reflected at the water surface. Most light is transmitted into the water. Due to refraction at the air-water boundary a ray with a solid angle of Ω above the water is focused into a smaller angle of Ω / n_w^2 below the water (n_w = refractive index of water), thus a radiance sensor with a small, but constant field of view detects more radiation below the water. Accounting for the loss $\sigma(\theta)$ at the surface and the gain $\sigma^-(\theta)$ from upwelling light L_u^- that is reflected back at the surface, the downwelling radi-

 <p>DLR Remote Sensing Technology Institute</p>	<p style="text-align: center;">ATBD Phytoplankton classification DRAFT</p>	<p>Doc. ID : MAPP-ATBD-PCLASS Name : Phytoplankton Classification Issue : Draft Rev.: 0 Date : 4.2.2000 Page : 5</p>
--	--	--

ance below the water surface is

$$L_d^-(\lambda, \theta') = (1 - \sigma(\theta)) \cdot n_w^2 \cdot L_d(\lambda, \theta) + \sigma^-(\theta') \cdot L_u^-(\theta'). \quad (3)$$

According to Snell's law the relation between the zenith angles above (θ) and below (θ') the water surface is $n_w \sin\theta = \sin\theta'$. By integration over all azimuth and zenith angles the following relation between the downwelling irradiance above (E_d) and below (E_d^-) the water surface is obtained:

$$E_d^-(\lambda) = (1 - \sigma) \cdot E_d(\lambda) + \sigma^- \cdot E_u^-(\lambda). \quad (4)$$

σ is an average reflection factor for specularly reflected radiation from the upper hemisphere, σ^- is the analogue for the lower hemisphere. Typical values of σ are 0.02 to 0.03 for clear sky and high solar elevation and 0.05 to 0.07 for clear sky and solar zenith angles below 45° and for overcast sky (Jerlov 1976, Preisendorfer and Mobley 1986). σ^- is in the range of 0.50 to 0.57 with a value of 0.54 being typical (Jerome et al. 1990, Mobley 1999).

The upwelling radiance L_u in air after crossing the boundary is calculated from the upwelling radiance in water L_u^- as follows:

$$L_u(\lambda, \theta) = (1 - \sigma^-(\theta')) / n_w^2 \cdot L_u^-(\lambda, \theta') + \sigma(\theta) \cdot L_d(\lambda, \theta). \quad (5)$$

The second term on the right side are the specular reflections that have been discussed in 3.1.1.1. By integration over all angles follows the relation between the upwelling irradiance above (E_u) and below (E_u^-) the water surface:


$$E_u(\lambda) = (1 - \sigma^-) \cdot E_u^-(\lambda) + \sigma \cdot E_d(\lambda). \quad (6)$$

The ratio $E_u(\lambda) / E_d(\lambda)$ is called albedo.

3.1.1.3 Reflection in the water

Radiation transfer in the water depends on the geometry of the illumination (position of sun, clouds, angular distribution of diffuse radiation) and on absorption, scattering and fluorescence properties of water and its constituents. Accurate models (e.g. Monte Carlo models) are capable of calculating radiance spectra for any depth and observation angle. In practice the achievable accuracy is limited by the knowledge about the optical properties of the relevant water constituents. For example, only little measurements exist concerning the angle dependency of scattering (phase function) of different suspended material, and as the size distribution is only rarely determined, calculations are also not very accurate.

In practice simple analytical models frequently substitute accurate, angle-resolved models. This is because the parameters required for a correct mathematical treatment are often not accurately known (e.g. phase functions) and computing time is quite high. As long as the knowledge of the optical properties of the relevant water constituents, and not the model approxima-

 <p>DLR Remote Sensing Technology Institute</p>	<p>ATBD Phytoplankton classification DRAFT</p>	<p>Doc. ID : MAPP-ATBD-PCLASS Name : Phytoplankton Classification Issue : Draft Rev.: 0 Date : 4.2.2000 Page : 6</p>
--	--	--

tions, limits the achievable accuracy, the use of a simple model is of advantage. As this is the case for remote sensing, the present algorithm for phytoplankton classification uses such a simple analytical model, namely the model of Gordon et al. (1975). It relates the irradiance reflectance R to the inherent optical properties a (absorption) and b_b (backscattering):

$$R(\lambda) = f \cdot \frac{b_b(\lambda)}{a(\lambda) + b_b(\lambda)}. \quad (7)$$

The factor of proportionality, f , depends on the scattering properties of the water and on the illumination and viewing geometry. There exist several algorithms to estimate f (Aas 1987, Kirk 1991, Sathyendranath and Platt 1997). Here $f = 0.33$ is set, which is a good approximation for clear sky conditions at high solar elevation (Gordon et al. 1975, Prieur 1976). In the inversion model the product of f with an other factor ρ^- is determined iteratively.

The spectra $a(\lambda)$ and $b_b(\lambda)$ depend on the dissolved and suspended water constituents. Their parameterisation is described below (3.1.1.4 and 3.1.1.5). The irradiance reflectance R is defined as the ratio of upwelling irradiance E_u^- to downwelling irradiance E_d^- , both measured below the water surface (labeled by a superscript "-"):

$$R(\lambda) = E_u^-(\lambda) / E_d^-(\lambda). \quad (8)$$

E_d is the integral of all radiances $L_d(\theta, \phi)$ downwelling from zenith angles $0 \leq \theta < 90^\circ$ and azimuth angles $0 \leq \phi < 360^\circ$, weighted with the cosine of the zenith angle:


$$E_d(\lambda) = \int_0^{2\pi} \int_0^{\pi/2} L_d(\lambda, \theta, \Phi) \cdot \cos\theta \cdot d\theta d\Phi. \quad (9)$$

$E_u(\lambda)$ is defined analogously, but the zenith angle ranges from $90^\circ < \theta \leq 180^\circ$.

Model (7) was developed for in-situ measurement of instruments that have a 180° field of view and measure irradiances. It is common use to apply it also to radiance measurements where the sensor has a narrow field of view. Measured upwelling radiances L_u are converted into irradiances E_u by multiplication with a factor Q , which depends on the scattering properties of the water. E_d can be determined with a radiance sensor using a white diffusor panel. If the reflection $r_p(\lambda)$ of the panel is isotropic (Lambertian reflector) and if it is kept horizontally, the radiance spectrum of the panel multiplied with $\pi/r_p(\lambda)$ yields $E_d(\lambda)$.

3.1.1.4 Absorption of water

The absorption of the water body is the sum of absorption of pure water, a_w , plus the absorption of all water constituents. In the visible and near infrared the main absorbing components are dissolved organic matter (yellow substance) and phytoplankton. Thus absorption can be expressed in good approximation by the following equation:

 <p>DLR Remote Sensing Technology Institute</p>	<p>ATBD Phytoplankton classification DRAFT</p>	<p>Doc. ID : MAPP-ATBD-PCLASS Name : Phytoplankton Classification Issue : Draft Rev.: 0 Date : 4.2.2000 Page : 7</p>
--	--	--

$$a(\lambda) = a_w(\lambda) + C_Y \cdot a_Y^*(\lambda) + \sum_P C_P \cdot a_P^*(\lambda). \quad (10)$$

C_Y and C_P denote the concentrations of yellow substance and phytoplankton, respectively, and $a_Y^*(\lambda)$ and $a_P^*(\lambda)$ their specific (i.e. normalized to concentration) absorption spectra. The specific absorption spectrum of yellow substance is approximately an exponential function:

$$a_Y^*(\lambda) = \exp[-S \cdot (\lambda - \lambda_0)]. \quad (11)$$

For Lake Constance the spectral slope has a typical value of $S = 0.0142 \text{ nm}^{-1}$. Yellow substance concentration is expressed as absorption at $\lambda_0 = 440 \text{ nm}$. Its mean value for Lake Constance is $C_Y = 0.29 \text{ m}^{-1}$.

The concentrations C_P of the phytoplankton classes are defined as mass of chlorophyll-a per volume and have the units $\mu\text{g/l}$. The specific absorption spectra $a_P^*(\lambda)$ of the optical phytoplankton classes have several characteristic peaks of approximate Gaussian shape. The peaks at 430 and 670 nm are present at all classes and vary not much in shape and amplitude, as these peaks are caused by chlorophyll-a which is present in all classes. The spectra $a_P^*(\lambda)$ representing the phytoplankton in Lake Constance are shown in the Appendix.

3.1.1.5 Backscattering of water


The backscattering coefficient of the water body is the sum of backscattering of pure water, $b_{b,w}$, plus the backscattering of all water constituents. For pure water the empirical relation of Morel (1974) is used:

$$b_{b,w}(\lambda) = b_1 \cdot \left(\frac{\lambda}{\lambda_1} \right)^{-4.32}. \quad (12)$$

The factor of proportionality, b_1 , depends on salinity. It is $b_1 = 0.00111 \text{ m}^{-1}$ for fresh water and $b_1 = 0.00144 \text{ m}^{-1}$ for typical oceanic water with a salinity of 35–38 ‰, if $\lambda_1 = 500 \text{ nm}$ is chosen as reference wavelength (Morel 1974).

Scattered intensities depend on the scattering angle and on particle size relative to λ , shape, refractive index and absorption. In the visible and near infrared the main scattering component is suspended matter. It is composed of inorganic and organic particles, mainly phytoplankton. Several published models use specific backscattering coefficients for a few components, for example for phytoplankton and the inorganic particles. However, these are highly variable, mainly due to the large natural variability of the size. For this reason, and because characteristic spectral features are missing, "class-specific" backscattering coefficients are much less specific than absorption spectra. In the model presented here no class-specific backscattering coefficients are used. Instead, the backscattering of all water constituents is approximated by the sum of a wavelength-independent term and a term proportional to λ^n :

$$b_b(\lambda) = b_{b,w}(\lambda) + C_L \cdot b_{b,L}^* + C_S \cdot b_{b,S}^* \cdot (\lambda/\lambda_S)^n. \quad (13)$$

 <p>DLR Remote Sensing Technology Institute</p>	<p style="text-align: center;">ATBD Phytoplankton classification DRAFT</p>	<p>Doc. ID : MAPP-ATBD-PCLASS Name : Phytoplankton Classification Issue : Draft Rev.: 0 Date : 4.2.2000 Page : 8</p>
--	--	--

Backscattering of particles with a diameter large compared to λ (above ca. 5 μm) is approximated by the product of concentration C_L and a wavelength-independent specific backscattering coefficient $b_{b,L}^*$. Scattering of smaller particles obeys approximately Ångström's (1929) empirical λ^n law, which follows from Mie theory for a size distribution of spherical particles proportional to d^{n-3} with d = diameter (van de Hulst 1957). Consequently, the backscattering of small particles is parameterised as the product of concentration C_S , specific backscattering coefficient $b_{b,S}^*$ at a reference wavelength λ_S , and the function $(\lambda/\lambda_S)^n$. For many water types $n = -1$ was observed to be a good approximation (Maffione and Dana 1997). For Lake Constance it is $b_{b,L}^* = 0.0086 \text{ m}^2 \text{ g}^{-1}$ and $b_{b,S}^* \approx 0$ (Heege 2000), i.e. backscattering of small particles can be neglected.

3.1.1.6 The analytic forward model

The analytic model (7) is used for parameterising the subsurface reflectance of the water. It eliminates the illumination conditions from the equation by normalising the information-bearing measurement of upwelling radiation with the downwelling irradiance. The same normalisation is performed for L_u measurements above the water surface:

$$r(\lambda) = \frac{L_u(\lambda)}{E_d(\lambda)}. \quad (14)$$

$E_d(\lambda)$ is the downwelling irradiance just above the water surface. Inserting the equations (4) and (5) and using $E_u^- = Q L_u^-$ yields the following expression:

$$r(\lambda) = \frac{(1-\sigma)(1-\sigma^-(\theta')) \cdot E_u^-(\lambda)}{Q \cdot n_w^2 \cdot E_d^-(\lambda) - \sigma^- \cdot E_u^-(\lambda)} + \frac{\sigma(\theta) \cdot L_d(\lambda, \theta)}{E_d(\lambda)}. \quad (15)$$


As irradiance reflectance is for most water types below 5 %, the denominator of the first term of the right-hand side approximately equals $E_d^-(\lambda)$, and it follows by using eq. (8):

$$r(\lambda) = \frac{(1-\sigma)(1-\sigma^-(\theta'))}{Q \cdot n_w^2} \cdot R(\lambda) + \sigma(\theta) \cdot \frac{L_d(\lambda, \theta)}{E_d(\lambda)}. \quad (16)$$

Since σ , $\sigma^-(\theta)$, $\sigma(\theta)$, Q and n_w depend only slightly on the wavelength, both terms on the right side can be approximated by products of wavelength-independent factors and wavelength-dependent functions:

$$r(\lambda) = \rho^- \cdot R(\lambda) + \rho^+ \cdot \frac{L_d^*(\lambda)}{E_d(\lambda)}. \quad (17)$$


The factors are in the orders of $\rho^- = 0.11 \text{ sr}^{-1}$ and $\rho^+ = 0.03$, because $\sigma \approx 0.02$, $\sigma^-(\theta) \approx 0.02$, $\sigma(\theta) \approx 0.03$, $Q \approx 5 \text{ sr}$, $n_w \approx 1.33$. The spectrum $L_d(\lambda, \theta)$ has been replaced by a spectrum

 DLR Remote Sensing Technology Institute	ATBD Phytoplankton classification DRAFT	Doc. ID : MAPP-ATBD-PCLASS Name : Phytoplankton Classification Issue : Draft Rev.: 0 Date : 4.2.2000 Page : 9
--	--	---

$L_d^*(\lambda)$, which represents a radiance spectrum that is reflected at a water-roughened surface into the sensor. As explained in Appendix A, it can be approximated by a sum of four base functions. In the forward model $L_d^*(\lambda)$ is calculated using user-defined weights α^* , β^* , γ^* , δ^* of the base functions, in the inversion model these weights are determined iteratively.

Eq. (17) is the analytic model which is used for forward and inverse calculations. Table 1 lists all parameters of eq. (17) and their default values. In the forward model the actual parameter values are set by the user, in the inversion model several of them are fit parameters and determined iteratively.

function	parameter	default value	meaning	remark
$R(\lambda)$	C_Y	0.29 m ⁻¹	yellow substance absorption at 440 nm	
	S	0.0142 nm ⁻¹	spectral slope of yellow substance absorption	not fitted
	C_{cl}	1 µg/l	cryptophyta concentration	low phycoerythrin concentration
	C_{ch}	1 µg/l	cryptophyta concentration	high phycoerythrin concentration
	C_d	1 µg/l	diatom concentration	
	C_{df}	1 µg/l	dinoflagellate concentration	
	C_g	1 µg/l	green algae concentration	
	C_L	2 mg/l	concentration of large particles	
	C_s	0	concentration of small particles	neglected for Lake Constance
	n	-1	Ångström exponent of backscattering by small particles	not fitted for Lake Constance
	f	0.33	factor of proportionality	not fitted
$L_d^*(\lambda)$	α^*	0.4	reflection factor of direct solar radiation	
	β^*	0.1	reflection factor of blue sky	
	γ^*	0.1	reflection factor of aerosol scattered radiation	
	δ^*	0.1	reflection factor of clouds	
	ν^*	0	Ångström exponent of aerosols	not fitted
$E_d(\lambda)$	α	0.4	weight of direct solar radiation	not fitted, but determined separately
	β	0.1	weight of radiation scattered by molecules	not fitted, but determined separately
	γ	0.1	weight of radiation scattered by aerosols	not fitted, but determined separately
	δ	0.1	weight of radiation scattered by clouds	not fitted, but determined separately
	ν	0	Ångström exponent of aerosols	not fitted
$r(\lambda)$	ρ^-	0.11 sr ⁻¹	conversion factor irradiance reflectance to remote sensing reflectance	

 DLR Remote Sensing Technology Institute	ATBD Phytoplankton classification DRAFT	Doc. ID : MAPP-ATBD-PCLASS Name : Phytoplankton Classification Issue : Draft Rev.: 0 Date : 4.2.2000 Page : 10
--	--	--

	ρ^+	0.03	reflection factor for sky radiances	
--	----------	------	-------------------------------------	--

Table 1: The parameters of the analytic model (17).

3.1.1.7 Inversion model for ship measurements

to be completed

3.1.1.8 Inversion model for MERIS

to be completed

3.1.2 Mathematical Description of the Algorithm

A detailed mathematical description is given together with a schematic description.

3.2 Practical Considerations

This section describes anticipated techniques for algorithm implementation. This section focusses on scientific issues involved in algorithm implementation.

3.2.1 Numerical computation considerations

3.2.2 Calibration and Validation

Validation methodologies shall be outlined.

3.2.3 Quality Control and Diagnostics

Quality control and diagnostics will be developed to inform the users of the uncertainties expected in the final results, for example, the effects of sub-pixel clouds and adjacent clouds.

3.2.4 Exception Handling


Actions on saturation or data dropouts shall be given.

Action on non-availability of ancillary and auxiliary data shall be given. The product(s) format will be described with their likely precision. Accompanying each product will be a summary of the input parameters used and an error budget. A data product summary sheet shall be produced (Chapter 7).

3.2.5 Output Product

4. Error Budget Estimates

An error budget on the uncertainties/errors described in the above section is given. The extend of validity is discussed, for example it's regional and seasonal applicability.

 <p>DLR Remote Sensing Technology Institute</p>	<p>ATBD Phytoplankton classification DRAFT</p>	<p>Doc. ID : MAPP-ATBD-PCLASS Name : Phytoplankton Classification Issue : Draft Rev.: 0 Date : 4.2.2000 Page : 11</p>
--	--	---

5. Assumptions and Limitations

Assumptions and limitations shall be summarized including assumptions on the quality of input data (L1b, L2 data, ancillary data, flags) required to achieve certain accuracy.


A major contribution to the signal at satellite height originates from the atmosphere; typically more than 90 %. Atmosphere correction procedures have been adapted to MERIS for land (Santer et al. 1997), case 1 waters (Antoine and Morel 1997) and case 2 waters (Aiken and Moore 1997). These procedures are implemented as standard software in ESA's MERIS processor. It is expected that the ESA software corrects the atmospheric influence with sufficient accuracy. Hence the proposed algorithm is based on full-resolution MERIS Level-2 data, i.e. normalized water leaving radiance (reflectance) spectra, for which ESA promises an accuracy $< 2 \times 10^{-4}$ (product ID: MER_FR_2P, see <http://envisat.estec.esa.nl/instruments/meris/data-app/prodsread.html>).

As it is not an easy task to correct accurately the atmospheric influence, it cannot be excluded that errors from atmosphere correction introduce errors into the determination of water constituents and phytoplankton classification.

It is planned to perform relevant calculations of error propagation.

6. References

- E. Aas (1987): Two-stream irradiance model for deep waters. *Applied Optics* 26(11), 2095-2101.
- J. Aiken, G. Moore (1997): ATBD Case 2 S Bright Pixel Atmospheric Correction. *Algorithm technical basis document 2.6*. ESA Doc. No. PO-TN-MEL-GS-0005.
- A. Ångström (1929). *Geograf. Ann.*, 11, 156. Cited in van de Hulst (1957).
- D. Antoine, A. Morel (1997): ATBD Atmosphere corrections above Case 1 Waters. *Algorithm technical basis document 2.7*. ESA Doc. No. PO-TN-MEL-GS-0005.
- E. H. Avrett (1997): Modeling solar variability - synthetic models. Solar Electromagnetic Radiation Study for Solar Cycle 22, Proceedings of the SOLERS22 Workshop held at the National Solar Observatory, Sacramento Peak, Sunspot, New Mexico, June 17-21, 1996. Edited by J. M. Pap, C. Frohlich, and R. K. Ulrich. Kluwer Academic Publishers, 1998., p.449. Also: http://cfa-www.harvard.edu/~avrett/genereview/gene_review.html
- C. Cox, W. Munk (1954): Statistics of the sea surface derived from sun glitter. *J. Marine Res.*, 13, 198-227.
- C. Cox, W. Munk (1956): Slopes of the sea surface deduced from photographs of sun glitter. *Bulletin Scripps Inst. Oceanogr. Univ. Calif.*, 6, 401-488.

 <p>DLR Remote Sensing Technology Institute</p>	<p>ATBD Phytoplankton classification DRAFT</p>	<p>Doc. ID : MAPP-ATBD-PCLASS Name : Phytoplankton Classification Issue : Draft Rev.: 0 Date : 4.2.2000 Page : 12</p>
--	--	---

P. Gege (1994): Gewässeranalyse mit passiver Fernerkundung: Ein Modell zur Interpretation optischer Spektralmessungen. *Dissertation. DLR-Forschungsbericht 94-15, 171 S.*

P. Gege (1998a): Correction of specular reflections at the water surface. *Ocean Optics XIV, November, 10-13, 1998, Kailua-Kona, Hawaii, USA. Conference Papers, Vol. 2.*

P. Gege (1998b): Characterization of the phytoplankton in Lake Constance for classification by remote sensing. *Arch. Hydrobiol. Spec. Issues Advanc. Limnol. 53, p. 179-193, Dezember 1998: Lake Constance, Characterization of an ecosystem in transition.*

P. Gege (1999): Lake Constance: Yellow substance measurements in 1998. *DLR Oberpfaffenhofen, IB 552-9/99, 17 p.*

H. R. Gordon, O. B. Brown, M. M. Jacobs (1975): Computed Relationships between the Inherent and Apparent Optical Properties of a Flat Homogeneous Ocean. *Applied Optics 14, 417-427.*

G. M. Hartmann (1995): Untersuchungen zum Absorptions- und Streuverhalten von Wasserinhaltsstoffen für die Auswertung von Fernerkundungsdaten. *Diplomarbeit am Lehrstuhl für Geographie und Hydrologie. Albert-Ludwigs-Universität Freiburg. 91 S.*

F. T. Haxo, D. C. Fork (1959): Photosynthetically Active Accessory Pigments of Cryptomonads. *Nature 184, 1051-1052.*

T. Heege, H. van der Piepen, J. Fischer, V. Amann (1998): Gewässerfernerkundung am Bodensee: Verfahren und Anwendungsbeispiele. *DLR Forschungsbericht 98-22.*

T. Heege (2000): Flugzeuggestützte Fernerkundung von Wasserinhaltsstoffen im Bodensee. *Dissertation. To be published in 2000.*

F. E. Hoge, P. E. Lyon (1996): Satellite retrieval of inherent optical properties by linear matrix inversion of oceanic radiance models: an analysis of model and radiance measurement errors. *J. Geophys. Res. 101, 16,631-16,648.*


N. G. Jerlov (1976): Marine Optics. *Elsevier Scientific Publ. Company.*

J. H. Jerome, R. P. Bukata, J. E. Bruton (1990): Determination of available subsurface light for photochemical and photobiological activity. *J. Great Lakes Res. 16(3), 436-443.*

J. T. O. Kirk (1991): Volumen scattering function, average cosines, and underwater lightfield. *Limnol. Oceanogr. 36, 455-467*

H. Krawczyk, A. Neumann, T. Walzel, G. Zimmermann (1993): Investigation of Interpretation possibilities of spectral high dimensional measurements by means of Principal Component Analysis - A concept for physical interpretation of those measurements. *SPIE Proceedings, Vol. 1938, 401-411.*

R. L. Kurucz (1992): Atomic and Molecular Data for Opacity Calculations; "Finding" the "Miss-

 <p>DLR Remote Sensing Technology Institute</p>	<p>ATBD Phytoplankton classification DRAFT</p>	<p>Doc. ID : MAPP-ATBD-PCLASS Name : Phytoplankton Classification Issue : Draft Rev.: 0 Date : 4.2.2000 Page : 13</p>
--	--	---

ing" Solar Ultraviolet Opacity; Remaining Line Opacity Problems for the Solar Spectrum, all in *Revista Mexicana de Astronomia y Astrofisica*, 23.

R. L. Kurucz (1994): The Solar Irradiance by Computation. Proc. of the 17th Annual Review Conference on Atmospheric Transmission Models, 7 June 1994, Geophysics Directorate/Phillips Laboratory.

R. A. Maffione, D. R. Dana (1997): Instruments and methods for measuring the backward-scattering coefficient of ocean waters. *Appl. Optics* 36, 6057-6067.

C. D. Mobley (1999): Estimation of the remote-sensing reflectance from above-surface measurements. *Appl. Optics* 38, 7442-7455.

A. Morel (1974): Optical Properties of Pure Water and Pure Sea Water. In: Jerlov, N. G., Steemann Nielsen, E. (Eds.): *Optical Aspects of Oceanography*. Academic Press London, 1-24.

H. Neckel, D. Labs (1981): Improved Data of Solar Spectral Irradiance from 0.33 to 1.25 μm . *Sol. Phys.* 74, 231-249.

R. W. Preisendorfer, C. D. Mobley (1986): Albedos and glitter patterns of a wind-roughened sea surface. *J. Phys. Oceanogr.* 16, 1293-1316.

L. Prieur (1976): Transfers radiatifs dans les eaux de mer. *Thesis, Doctorat d'Etat, Univ. Pierre et Marie Curie, Paris*, 243 pp.

R. Santer, V. Carrère, D. Dessailly, P. Dubuisson, J.-C. Roger (1997): ATBD Atmosphere corrections above land. *Algorithm technical basis document 2.15*. ESA Doc. No. PO-TN-MEL-GS-0005.


S. Sathyendranath, T. Platt (1997): Analytic model of ocean color. *Applied Optics* 36, 2620-2629

H. Schiller, R. Doerffer (1993): Fast computational scheme for inverse modelling of multispectral radiances: application for remote sensing of the ocean. *Applied Optics* 32, 3280-3285.

R. C. Smith, K. S. Baker (1981): Optical properties of the clearest natural waters (200-800 nm). *Applied Optics* 20, 177-184 (1981).

H. C. van de Hulst (1957): Light scattering by small particles. *Wiley, New York*. 470 pp.

W. von Smekot-Wensierski, B. Wozniak, H. Graßl, R. Doerffer (1992): Die Absorptionseigenschaften des marinen Phytoplanktons. *GKSS Forschungszentrum Geesthacht, Bericht Nr. 92/E/105*, 104 p.

 Remote Sensing Technology Institute	ATBD Phytoplankton classification DRAFT	Doc. ID : MAPP-ATBD-PCLASS Name : Phytoplankton Classification Issue : Draft Rev.: 0 Date : 4.2.2000 Page : 14
--	--	--

Appendix A: An analytic model of the downwelling radiation

An analytic model of the downwelling radiation with only few parameters has been developed by Gege (1994). The actual version is described here. Its main purpose is to correct specular reflections at the water surface. These cannot be calculated with sufficient accuracy with an "exact" angle-resolved model (like Modtran, 6S etc.), because for a wind-roughened water surface the reflected region of the upper hemisphere is statistically fluctuating. Higher accuracy is achieved by adjusting the few parameters of the analytic model in an inverse procedure (Gege 1998a).

A.1 The model


The parameterisation of the downwelling radiation is based on the fact that the radiation illuminating the water surface consists of four spectrally different components: (1) the direct solar radiation transmitted through the atmosphere, (2) the blue sky, (3) radiation scattered by aerosols, and (4) clouds. Each component is expressed in terms of a wavelength-dependent fraction of the extraterrestrial solar irradiance $E_0(\lambda)$:

$$E_d(\lambda) = [\alpha \cdot t_A(\lambda) + \beta \cdot (\lambda/\lambda_R)^{-4.09} + \gamma \cdot (\lambda/\lambda_M)^v + \delta \cdot t_C(\lambda)] \cdot E_0(\lambda). \quad (\text{A.1})$$

This is the defining equation of the four base functions $t_A(\lambda)$, $(\lambda/\lambda_R)^{-4.09}$, $(\lambda/\lambda_M)^v$ and $t_C(\lambda)$. Accordingly the base functions are a ratio of two irradiance spectra, hence they are diffuse transmission spectra. In order to make them all dimensionless, the constants λ_R and λ_M are introduced, whose values are determined by normalisation. The relative intensity of each base function – α , β , γ and δ – may change from one measurement to the other, but the base functions themselves are assumed to be constant in time.

The assumption behind eq. (A.1) is that each point of the sky emits radiation which is a weighted sum of the four light sources sun, blue sky, aerosols and clouds. Hence eq. (A.1) is as well a model for the downwelling irradiance $E_d(\lambda)$ as also for the downwelling radiance $L_d(\lambda, \theta, \phi)$ for any zenith angle $0 \leq \theta < 90^\circ$ and any azimuth angle $0 \leq \phi < 360^\circ$. In particular it is a suitable model for the radiation which is specularly reflected at the water surface. Accordingly the radiance spectrum $L_d^*(\lambda)$ of eq. (17) is parameterised as follows:

$$L_d^*(\lambda) = [\alpha^* \cdot t_A(\lambda) + \beta^* \cdot (\lambda/\lambda_R)^{-4.09} + \gamma^* \cdot (\lambda/\lambda_M)^v + \delta^* \cdot t_C(\lambda)] \cdot E_0(\lambda). \quad (\text{A.2})$$

 <p>DLR Remote Sensing Technology Institute</p>	<p>ATBD Phytoplankton classification DRAFT</p>	<p>Doc. ID : MAPP-ATBD-PCLASS Name : Phytoplankton Classification Issue : Draft Rev.: 0 Date : 4.2.2000 Page : 15</p>
--	--	---

A.2 The light sources

The base spectra $t_A(\lambda)$, $(\lambda/\lambda_R)^{-4.09}$, $(\lambda/\lambda_M)^v$ and $t_C(\lambda)$ of the model (A.1) represent the four light sources sun, blue sky, aerosols and clouds, respectively. Their calculation is described below. They are shown in Fig. A.1.

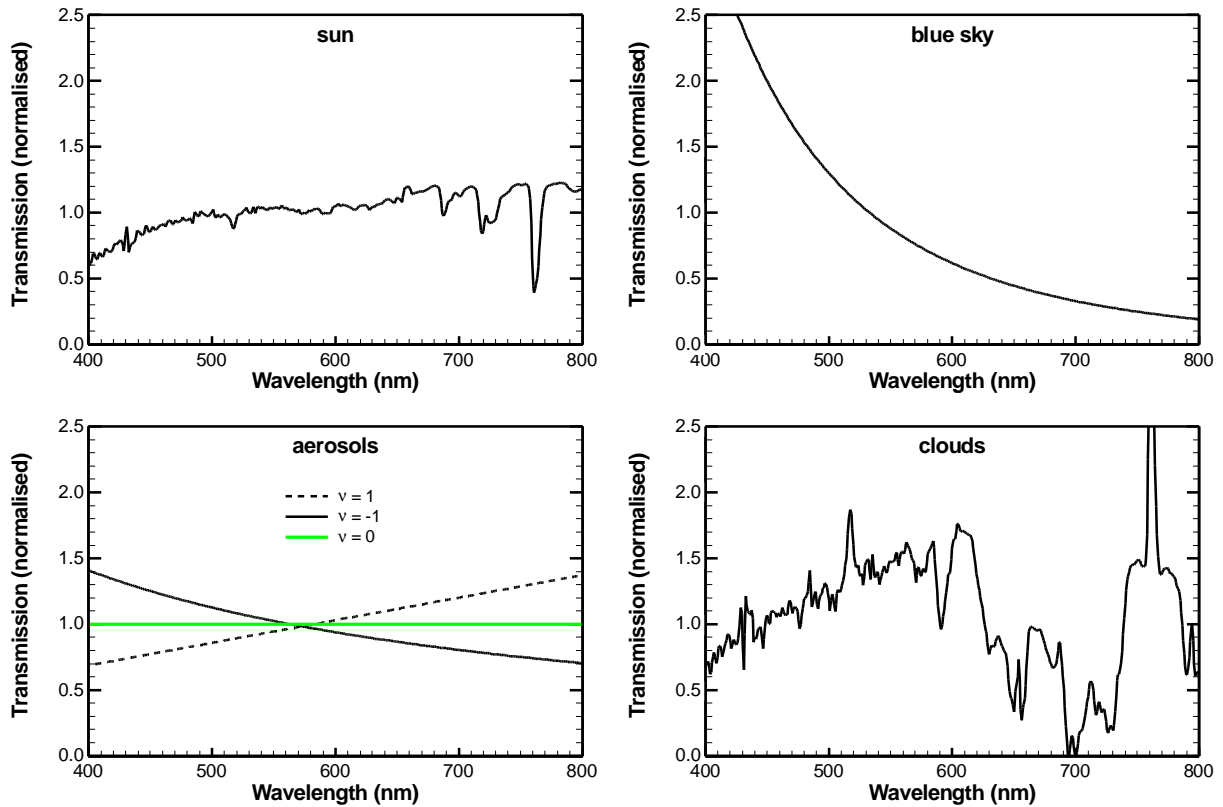



Fig. A.1: The four base spectra of the model of the downwelling radiation.

The transmission spectra of Fig. A.1 are normalised such that the weights α , β , γ and δ represent the relative intensities of the four light sources in the spectral range of 400 to 800 nm for an $E_d(\lambda)$ spectrum. This requirement corresponds to the following normalisation condition:

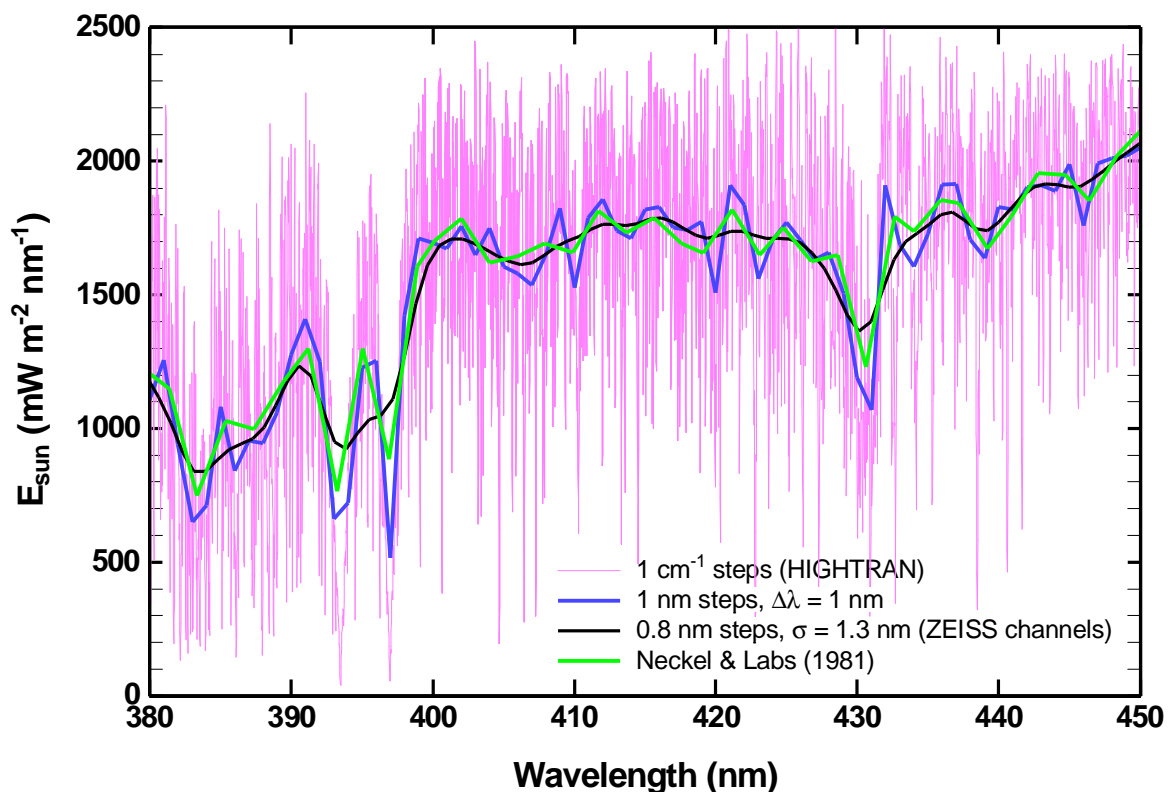
$$\int_{400}^{800} t_i(\lambda) \cdot E_0(\lambda) d\lambda = \int_{400}^{800} E_0(\lambda) d\lambda, \quad (\text{A.3})$$

with $t_i(\lambda) = t_A(\lambda)$, $(\lambda/\lambda_R)^{-4.09}$, $(\lambda/\lambda_M)^v$, $t_C(\lambda)$. From this equation the Rayleigh and Mie scaling factors are obtained: $\lambda_R = 533$ nm, λ_M depends on v : $\lambda_M = 583$ nm for $v = 1$ and $\lambda_M = 563$ nm for $v = -1$.

A.2.1 Extraterrestrial solar irradiance

 <p>DLR Remote Sensing Technology Institute</p>	<p>ATBD Phytoplankton classification DRAFT</p>	<p>Doc. ID : MAPP-ATBD-PCLASS Name : Phytoplankton Classification Issue : Draft Rev.: 0 Date : 4.2.2000 Page : 16</p>
--	--	---


The electromagnetic radiation from the sun is emitted by the solar photosphere. Its spectrum consists of millions of absorption and emission lines with temperature dependent line shape parameters. Models of the solar photosphere are derived semi-empirically by solving the equations describing the physical processes in the solar atmosphere as far as possible, and then adjusting atmospheric parameters to obtain agreement between calculated and observed intensities (Avrett 1997). In this way a compilation of more than 58 million atomic and molecular lines was performed by Kurucz (1992, 1994) and a spectrum of the solar irradiance with a resolution of 1 cm^{-1} was derived. Fig. A.2 shows this solar irradiance spectrum for the wavelength range of 380 to 450 nm together with three spectra which are averaged for spectrometers with a spectral resolution around 1 to 2 nm.



SOLAR | 4.11.1999

Fig. A.2: Comparison of solar irradiance spectra with different spectral resolutions.

The highly resolved data of Kurucz are included in the HITRAN database (<http://www.HITRAN.com>). One curve of Fig. A.2 was calculated from these 1 cm^{-1} data in 1 nm steps by integrating over intervals of $\pm 0.5 \text{ nm}$, corresponding to channels with rectangular response function and widths of $\Delta\lambda = 1 \text{ nm}$. An other curve was calculated from the 1 cm^{-1} data to match the channels of a ZEISS MCS 501 UV-NIR spectrometer owned by DLR. The spectral

 <p>DLR Remote Sensing Technology Institute</p>	<p>ATBD Phytoplankton classification DRAFT</p>	<p>Doc. ID : MAPP-ATBD-PCLASS Name : Phytoplankton Classification Issue : Draft Rev.: 0 Date : 4.2.2000 Page : 17</p>
--	--	---

response of each channel was assumed to have a Gaussian shape and a standard deviation of $\sigma = 1.3$ nm; the centre wavelengths (spacing 0.8 nm) were taken from the manufacturer's calibration table. The third curve is a frequently used spectrum of the solar irradiance that was measured by Neckel and Labs (1981) in steps of 2 nm and a spectral resolution around 2 nm.

Fig. A.2 clearly illustrates that a weighted integral of the solar irradiance over a certain wavelength range depends strongly on the weighting function and on the integral borders. Since any spectrometer integrates and weights the radiation over a certain wavelength range, the spectral response of all channels must be known very precisely if the instrument is used to measure solar radiation in absolute units, for example to derive a transmission spectrum.

The instrument-adapted spectrum with 0.8 nm steps and $\sigma = 1.3$ nm is taken as spektrum $E_0(\lambda)$ for the above-described model. This spectrum is shown for the spectral range of 400 to 800 nm in Fig. A.3. As explained below, the transmission spectra "sun" and "clouds" of Fig. A.1 have been derived from experimental data with the $E_0(\lambda)$ spectrum of Fig. A.3 as light source. The remaining spectral mismatch between the instrument and $E_0(\lambda)$ causes the "noise" that is visible in the transmission spectra.

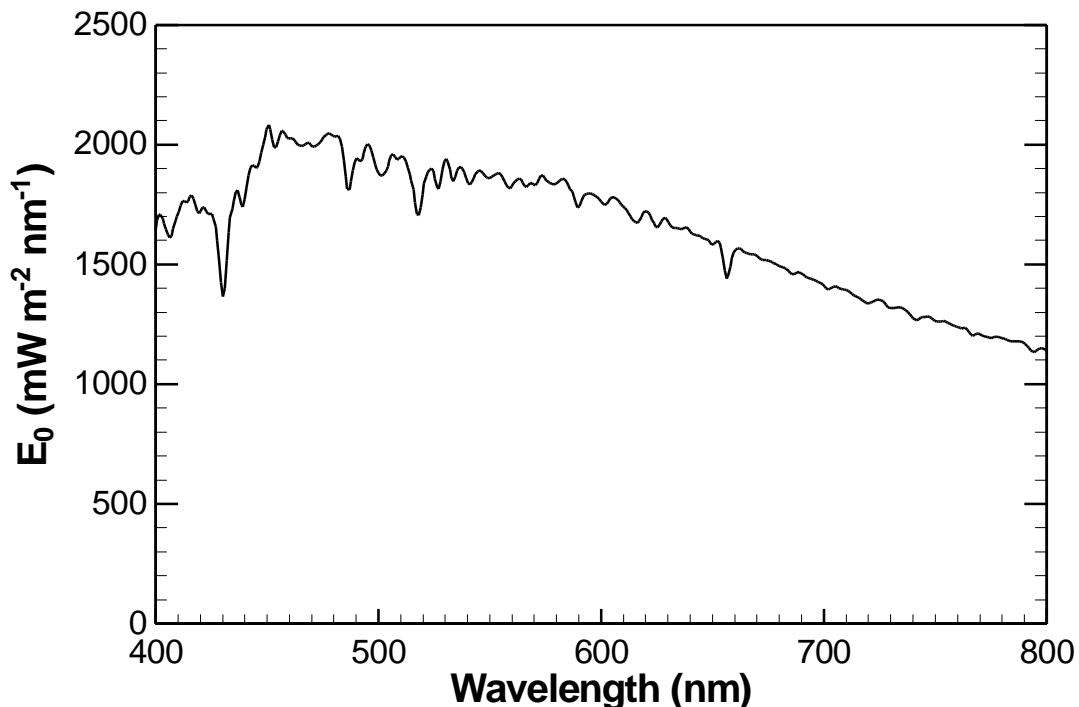



Fig. A.3: Extraterrestrial solar irradiance spectrum $E_0(\lambda)$.

A.2.2 Direct solar transmission

 <p>DLR Remote Sensing Technology Institute</p>	<p>ATBD Phytoplankton classification DRAFT</p>	<p>Doc. ID : MAPP-ATBD-PCLASS Name : Phytoplankton Classification Issue : Draft Rev.: 0 Date : 4.2.2000 Page : 18</p>
--	--	---

The base spectrum $t_A(\lambda)$ was determined as follows. First an approximation $t'_A(\lambda)$ was calculated using the radiative transfer code Lowtran-7 (Kneizys et al., 1988). This spectrum was then used in eq. (A.1) for determining the parameters α , β , γ and ν in a least-squares fit by adjusting the right-hand side of eq. (A.1) to an $E_d(\lambda)$ measurement at cloud-free conditions ($\delta = 0$). Finally $t_A(\lambda)$ was calculated from eq. (A.1) using the fitted values of α , β , γ and ν . Several of these spectra were calculated from measurements at Lake Constance. That one was selected which was least influenced by water vapour absorption at 720 nm.

A.2.3 Blue sky

Light scattering by molecules obeys Rayleigh's classical λ^{-4} law (Strutt 1871). For the atmosphere this λ^{-4} -dependency is not strictly valid due to wavelength-dependent refraction. From experimental data several empirical relationships have been derived, which yield similar spectra. Here the empirical power law of Linke (1956) with an exponent of -4.09 is adopted.


A.2.4 Aerosols

For aerosol scattering the empirical λ^ν formula of Ångström (1929) is taken as base function. It follows from Mie theory for a size distribution of spherical particles proportional to d^{v-3} with d = diameter (van de Hulst 1957).

The model accuracy is not affected significantly by an incorrect Ångström exponent (Gege 1994). This behaviour of the model results from the method for calculating $t_A(\lambda)$: the method described in A.2.2 compensates errors in ν by errors in $t_A(\lambda)$. Consequently, actual measurements $E_d(\lambda)$ can be reproduced quite well as long as aerosol scattering has a similar wavelength dependence as for the measurement used for deriving $t_A(\lambda)$.

A.2.5 Clouds

The spectrum $t_C(\lambda)$ was determined from an $E_d(\lambda)$ measurement at overcast sky as follows. Since no first guess of $t_C(\lambda)$ existed, $t_C(\lambda) = 0$ was set in a first step, hence the only unknowns of eq. (A.1) are the parameters α , β , γ , ν , while all wavelength-dependent functions are known. These parameters were determined in a least-squares fit. From the difference between measurement $E_d(\lambda)$ and fit curve $f(\lambda)$ a first estimate of $t_C(\lambda)$ was calculated: $\delta \cdot t_C(\lambda) = [E_d(\lambda) - f(\lambda)] / E_0(\lambda)$. It contains negative and positive values. By adding the lowest t_C value to all spectral channels a new spectrum $t_C(\lambda)$ was obtained which contains only positive values. Its scaling factor δ was determined by normalisation according to eq. (A.3). This spectrum $t_C(\lambda)$ was then used in the next step to determine an improved parameter set α , β , γ , δ , ν by a least-squares fit, and these values were used to calculate a further improved spectrum $t_C(\lambda)$ with eq. (A.1). Several of these spectra were calculated from measurements at Lake Constance. That one was selected

 Remote Sensing Technology Institute	ATBD Phytoplankton classification DRAFT	Doc. ID : MAPP-ATBD-PCLASS Name : Phytoplankton Classification Issue : Draft Rev.: 0 Date : 4.2.2000 Page : 19
--	--	--

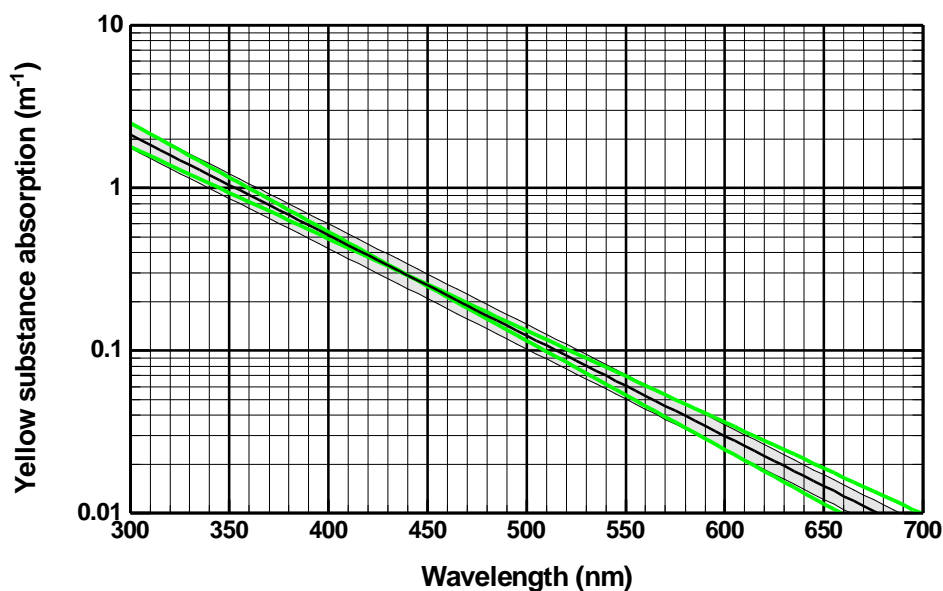
which was most influenced by water vapour absorption at 720 nm.

Appendix B: Optical properties of Lake Constance

The experimental basis of the algorithm are data from Lake Constance (Bodensee). These are summarized here.

B.1 Yellow substance

Yellow substance absorption and its variability have been studied during campaigns in May and September 1998. The measurements and the results are described in detail in Gege (1999). The major results are shown in Fig. B.1.




A_YS / 2.12.1999

Fig. B.1: Typical yellow substance absorption of Lake Constance. Bold: Mean spectrum. Gray shaded: standard deviation due to concentration changes. Green lines: standard deviation due to changes of the spectral slope.

The average absorption at 440 nm of samples from the lake is 0.29 m^{-1} . Significantly higher values are observed only in the Schussen river plume. Otherwise, the standard deviation of $a_Y(\lambda)$ due to concentration changes is 0.05 m^{-1} at 440 nm or $\pm 17 \%$. It is shown in Fig. B.1 as gray shaded area.

The spectral slope has a mean value of $S = 0.0142 \text{ nm}^{-1}$ and a standard deviation of 0.0012 nm^{-1} , which corresponds to a variability of $\pm 8 \%$. The resulting variability of yellow substance absorption $a_Y(\lambda)$ is shown in Fig. B.1 as green lines.

Scattering by yellow substance was not investigated. It is neglected in the model.

 <p>DLR Remote Sensing Technology Institute</p>	<p>ATBD Phytoplankton classification DRAFT</p>	<p>Doc. ID : MAPP-ATBD-PCLASS Name : Phytoplankton Classification Issue : Draft Rev.: 0 Date : 4.2.2000 Page : 21</p>
--	--	---

B.2 Phytoplankton

The model treats the phytoplankton in two ways: for correcting specular reflections at the water surface an average absorption spectrum is used, for phytoplankton classification the specific absorption spectra of all relevant optical classes are required. Backscattering of phytoplankton is lumped together in the model with backscattering of other suspended matter, i.e. no phytoplankton-specific backscattering spectra are required.

B.2.1 Average absorption spectrum

The average specific absorption spectrum of phytoplankton is shown in Fig. B.2. It is based on 213 reflectance measurements from 32 days in 1990 and 1991. By inverse modelling the phytoplankton absorption spectra have been derived (Gege 1994). These calculated in-situ absorption spectra have been normalized to the sum of chlorophyll-a and phaeophytin-a concentration. Heege (2000) has shown that this mean specific absorption spectrum is well-suited to derive the chlorophyll-a concentration from airborne data (DAEDALUS scanner) and from underwater reflectance spectra (MER radiometer).

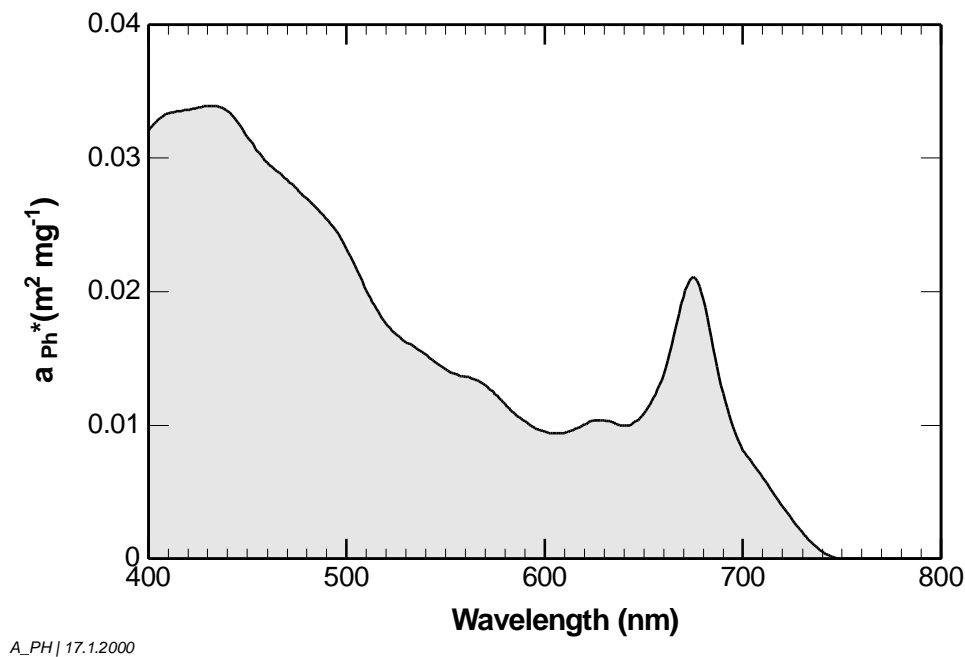


Fig. B.2: Mean specific absorption of phytoplankton in Lake Constance.

The spectrum of Fig. B.2 is used for correcting specular reflections at the water surface. This algorithm is not sensitive on minor deviations of the actual absorption spectrum from the mean spectrum. It excludes the spectral range from 500 to 600 nm where the deviations are largest.

B.2.2 Absorption spectra of major optical classes

The phytoplankton in Lake Constance is composed of more than hundred species. A spectral distinction on species level is not possible. Because all species belonging to the same taxonomic class contain similar pigment types, optical classification is oriented on taxonomic classification. Taxonomic classes which have similar absorption spectra are merged together into one optical class. A comparison of various measured and published spectra on species level led to the classification of Table B.1 (Gege 1994).

Taxonomic classes	Optical class
Cryptophyceae	cryptophyta
Bacillariophyceae Chrysophyceae	diatoms
Chlorophyceae Zygnemaphyceae Cyanophyceae	green algae
Dinophyceae	dinoflagellates

Table B.1: Optical classification of the phytoplankton in Lake Constance.

The classification of Table B.1 is based on laboratory measurements at pure cultures of single species. For two taxonomic classes the optical classification is not statistically proven:

- *Chrysophyceae*. Not a single absorption measurement was available. The class was put into the diatoms class because inversion of reflectance measurements determined high diatom concentrations for the two days when Chrysophyceae were dominating.
- *Cyanophyceae*. The absorption of many species belonging to this class is highly dependent on the illumination conditions during growth, and there are large differences between the species. For Lake Constance only one species, *Microcystis*, occurred at high concentrations, but the absorption spectrum of this species is not known. The class was put into the green algae class because inversion of reflectance measurements determined high green algae concentrations for the days when *Microcystis* was dominating.

The specific absorption spectra of the four optical phytoplankton classes are shown in Fig. B.3.

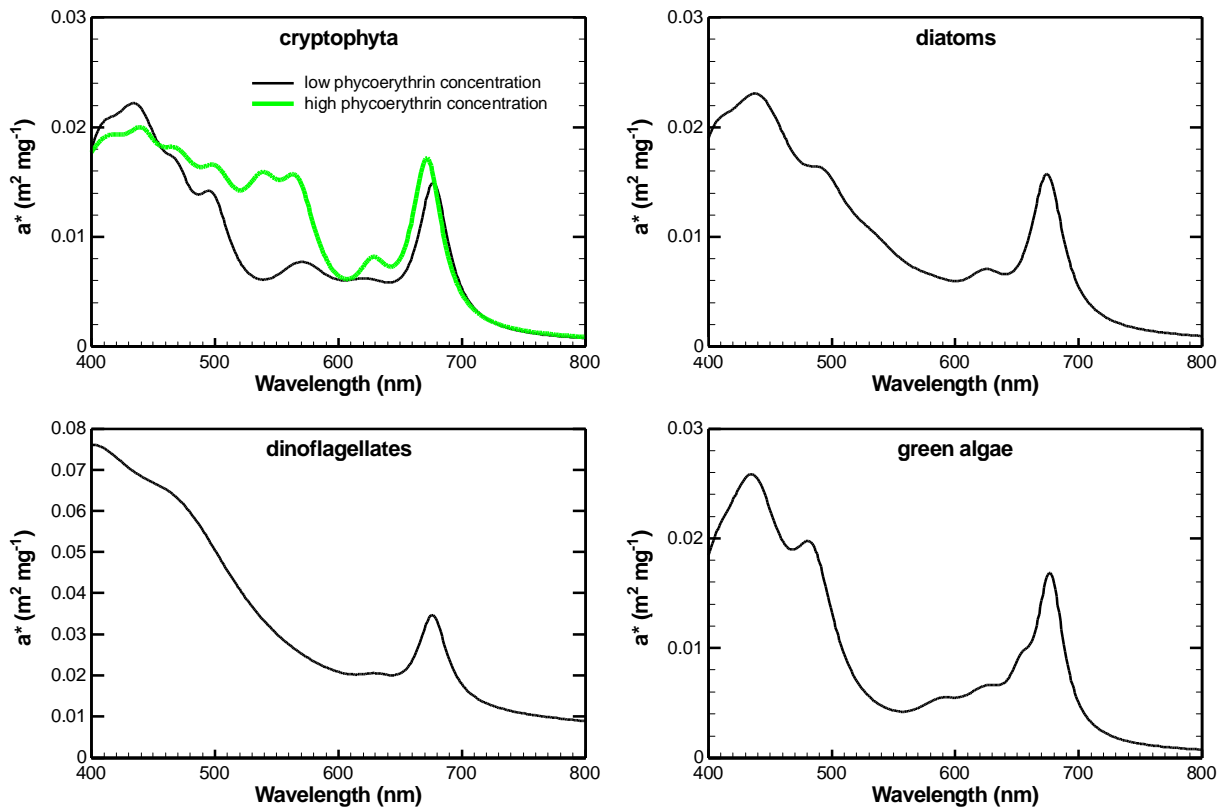



Fig. B.3: Specific absorption of the optical classes of the phytoplankton in Lake Constance. For cryptophyta two spectra are required to account for the high variability of the concentration of the pigment phycoerythrin.

For cryptophyta two spectra are required to account for the high variability of the pigment phycoerythrin. The spectrum which represents the class at low phycoerythrin concentration was measured (Hartmann 1995) on a pure culture of *Cryptomonas ovata*, which is by far the most abundant species in Lake Constance. To account for high phycoerythrin concentration a published (Haxo and Fork 1959) absorption measurement of the species *Rhodomonas lens* was digitized and re-scaled to $a^*(440) = 0.02 \text{ m}^2/\text{mg}$. For representing the specific absorption spectrum of diatoms a *Fragilaria crotonensis* measurement (Hartmann 1995) was chosen, for green algae a *Mougeotia sp.* measurement (Hartmann 1995), and for dinoflagellates a published spectrum (von Smekot-Wensierski et al. 1992) which averages five marine species.

B.3 Suspended matter

The specific absorption of suspended matter was calculated from underwater measurements of irradiance reflectance (139 depth profiles) and diffuse attenuation (142 depth profiles) at 88 days from 1990 to 1996. Two methods, multivariate optimisation and least-squares fit,

 Remote Sensing Technology Institute	ATBD Phytoplankton classification DRAFT	Doc. ID : MAPP-ATBD-PCLASS Name : Phytoplankton Classification Issue : Draft Rev.: 0 Date : 4.2.2000 Page : 24
--	--	--

were applied to the data set which comprises besides optical also biochemical measurements (Heege 2000). The result is that absorption of non-phytoplankton suspended matter is negligible.

The specific backscattering of suspended matter was determined by inverse modelling of 139 subsurface irradiance reflectance measurements from 1990 to 1996 in 1 m depth, for which the concentrations of inorganic and organic suspended matter, phytoplankton and yellow substance were known (Heege 2000). Because no clear distinction between the contributions of phytoplankton and inorganic matter was possible, the backscattering of all suspended particles is treated as an entity. It resulted no significant wavelength dependency of backscattering. The average specific backscattering coefficient of suspended matter is:

$$b_{b,L}^*(\lambda) = 0.0086 \text{ m}^2 \text{ g}^{-1}.$$

In accordance with eq. (13) the subscript "L" is used in order to indicate that backscattering is dominated by "large" particles. The natural variability of $b_{b,L}^*$ was estimated by comparing suspended matter concentrations derived from inversion of multispectral airborne data from 4 campaigns in 1996 and 1997 and in-situ measurements (Heege 2000). If water with very high concentrations near to river mouths is excluded, the average deviation is 25 %. Because part of the deviation is caused by other error sources, it can be concluded that the variability of $b_{b,L}^*$ in the lake is below 25 %.

Both results, the approximate independency from wavelength and the value around $0.01 \text{ m}^2 \text{ g}^{-1}$, were confirmed by direct measurements of the backscattered light. These measurements were performed in May and September 1998 with a commercial instrument (bb-4, Sequoia Scientific, owned by GKSS Geesthacht) that detects the light backscattered at an angle of 140° at 4 spectral channels at 414, 440, 510 and 675 nm.